

## Quantum theory of nondegenerate multiwave mixing

Seng-Tiong Ho, Prem Kumar,\* and Jeffrey H. Shapiro

Research Laboratory of Electronics, Massachusetts Institute of Technology, Cambridge, Massachusetts 02139

(Received 20 October 1986)

A quantum theory of nondegenerate multiwave mixing in a two-level atomic medium is formulated, with emphasis on traveling-wave interaction geometries. Two equivalent alternative methods are developed to treat, with some rigor, the spatial propagation of the interacting multimode traveling-wave field. The theory is applied to the case of a single beam propagating through the medium to obtain the spectrum of squeezing. The effects of spontaneous emission, propagation loss, atomic collisions, and pump-probe phase mismatch are comprehensively taken into account for the first time.

In this Rapid Communication, we summarize our formulation of a quantum theory for nondegenerate multiwave mixing in an atomic medium, and we report its application to traveling-wave squeezed-state generation experiments via four-photon mixing in such a medium.<sup>1</sup> The theory predicts squeezing in resonance fluorescence,<sup>2</sup> degenerate four-wave mixing,<sup>3</sup> and nondegenerate four-wave mixing<sup>4</sup> in a consistent manner. The effects of spontaneous emission, propagation loss, atomic collisions, and pump-probe phase mismatch on squeezing are properly taken into account. A preliminary analysis of the effect of superradiance has also been carried out.

In the frequency-degenerate limit, without consideration of pump-probe phase mismatch, our theory agrees with the earlier work of Reid and Walls,<sup>3</sup> and in the thin-medium approximation it correctly reproduces the results of Heidmann and Reynaud.<sup>2</sup> Recently, other<sup>4</sup> quantum theories for nondegenerate four-photon mixing have been developed and applied to intracavity atomic-beam squeezed-state generation experiments.<sup>5</sup> Our formulation, besides giving a more general expression for the atomic polarizability, differs from theirs in an essential way in that we handle the slowly-varying-amplitude approximation in the frequency domain. This approach more rigorously justifies the adiabatic approximation for the elimination of atomic variables, and leads to extra terms which are important for a consistent treatment of spatial propagation. Instead of adopting the heuristic  $t \rightarrow z/c$  transformation used in almost all the previous works, we have developed two equivalent methods to treat with some rigor the spatial propagation of a multimode traveling-wave field. The slowly varying-envelope method places a much better limit on the validity of the squeezed-noise calculations using the  $t \rightarrow z/c$  transformation,<sup>3</sup> whereas the quantum-mode method provides physical insight into how the time evolution of the usual annihilation operators leads to spatial propagation of the wave. Our inclusion of pump-probe phase mismatch, collisions, and superradiance also gives rise to additional effects not considered elsewhere.

In this theory, we consider a system of  $N$  stationary two-level atoms, uniformly distributed over a volume  $V_M$ , interacting with an infinite number of electromagnetic field modes quantized with periodic boundary conditions in a box of volume  $V_Q \gg V_M$ . We consider the explicit dy-

namics of  $q$  of these modes, leaving the rest as a common thermal-field reservoir for all atoms; this is physically realistic, and gives additional decay and fluctuation to the atomic variables due to cooperative behavior. Soft collisions between the atoms are modeled by coupling each atom to a separate phase-damping reservoir.

For this system, under dipole and rotating-wave approximations, we can derive the following set of  $c$ -number Langevin equations for the atomic variables using standard techniques:<sup>6</sup>

$$\frac{\partial V_i}{\partial t} = -a_{\mathbf{r}_i}(t)[n_{g_i} - n_i] - i\omega_a V_i - \gamma_{\perp} V_i - \sum_{i'(\neq i)} \gamma_{ii'}(n_{g_i} - n_i) V_i + f_{V_i}, \quad (1)$$

$$\frac{\partial n_i}{\partial t} = -a_{\mathbf{r}_i}^+(t) V_i - a_{\mathbf{r}_i}(t) V_i^+ - \gamma_{\parallel} n_i - \sum_{i'(\neq i)} \gamma_{ii'}(V_i^+ V_{i'} + V_{i'}^+ V_i) + f_{n_i}. \quad (2)$$

Here  $\omega_a$  is the atomic resonance frequency,  $n_{g_i} = 1 - n_i$ ,  $V_i$  and  $n_i$  are the  $c$ -number atomic down transition and upper-level occupation variables, respectively, for the  $i$ th atom, and

$$a_{\mathbf{r}_i}(t) = \sum_{j=1}^q C_j(\mathbf{r}_i) a_j(t)$$

gives the multimode field variable in terms of the coupling coefficients  $\{C_j(\mathbf{r}_i)\}$  for the  $j$ th mode to the atom at  $\mathbf{r}_i$  and the  $c$ -number variables  $\{a_j(t)\}$  for the field modes. The terms proportional to  $\gamma_{ii'}$  contribute extra damping to the  $i$ th atom due to collective spontaneous decay arising from the dipole phase coherence of the  $i$ th atom with the rest of the atoms. When the atomic medium is saturated by a pump mode with wave vector  $\mathbf{k}_p$  then these superradiance terms are negligible when either (a) the number of atoms in a diffraction volume  $N_D = \lambda_p^2 L_M N / V_M \ll 1$ , where  $\lambda_p \equiv 2\pi/|\mathbf{k}_p|$ , and  $L_M$  is the medium length, or (b) the atoms are off-resonantly pumped so that  $|(|\mathbf{k}_p| - \omega_a/c)| L_M \gg N_D$ . With collisions, the transverse relaxation rate  $\gamma_{\perp}$  is related to the longitudinal relaxation rate  $\gamma_{\parallel}$  via  $\gamma_{\perp} = \gamma_p + \gamma_{\parallel}/2 \equiv \gamma_{\parallel}/2F$  with  $0 \leq F \leq 1$ , where  $\gamma_p$  is the collisional dephasing rate.  $F=1$  corresponds to no collisions.

Neglecting the superradiance terms,

$$\begin{aligned} \langle f_{V_i}(t)f_{V_i}(t') \rangle, \quad \langle f_{n_i}(t)f_{n_i}(t') \rangle, \\ \langle f_{n_{gr}}(t)f_{n_{gr}}(t') \rangle = -\langle f_{n_i}(t)f_{n_{gr}}(t') \rangle \\ = \langle f_{n_i}(t)f_{n_i}(t') \rangle, \end{aligned}$$

and

$$\langle f_{V_i^+}(t)f_{V_i}(t') \rangle$$

are the only nonzero Langevin-noise correlations. All are proportional to  $\delta(t-t')\delta_{ii'}$ , with the first factor due to the usual Markov approximation, and the second to our assuming a zero-temperature thermal reservoir. The  $\delta$ -function coefficients are similar in form to those in the degenerate theory.<sup>3</sup>

Equations (1) and (2) can be solved by Fourier decomposition using series expansions for the field variables

$$a_{r_i}(t) = \sum_{k=1}^{\infty} A_k \exp(-i\nu_k t),$$

and Fourier transforms for the atomic variables and the noise forces, e.g.,

$$n_{r_i}(t) = \int_{-\infty}^{\infty} d\omega n_{r_i}(\omega) \exp(-i\omega t).$$

This procedure gives us an infinite set of coupled equations for  $n_{r_i}(\omega - \nu_k)$ , which can be solved iteratively to give  $n_{r_i}(\omega)$  as a power-series expansion in the Fourier coefficients  $\{A_k\}$ . This power series converges under certain circumstances, e.g., when the pump modes are strong and degenerate in frequency, whereas the other nondegenerate modes are weak.

Further, assuming that  $a_{r_i}(t)$  can be approximated by  $q$  slowly varying amplitudes  $\{a_j(t)\}$  related to  $\{a_j(t)\}$  via

$$a_j(t) = a_j(t) \exp(-i\omega_j' t),$$

we can solve for the atomic transition (or polarization) variable  $V_{r_i}(t)$  in terms of  $\{a_j(t)\}$  and their first derivatives  $\{(d/dt)a_j(t)\}$  under the approximation that  $\{a_j(t)\}$  do not change substantially during the characteristic relaxation time  $1/\gamma_{\perp}$  of the atoms. The first-derivative terms are essential to properly account for the refractive index and the group velocity of wave propagation. The solution for  $V_{r_i}(t)$ , thus obtained, consists of a deterministic part and a Langevin-noise part which is no longer  $\delta$ -function correlated in time, but shows the spectrum of resonance fluorescence.

Substituting  $V_{r_i}(t)$  into the Langevin equations for the field modes, we obtain a set of temporal coupled-mode equations for  $\{a_j(t)\}$ ,

$$\begin{aligned} \frac{\partial a_j}{\partial t} = -i(\omega_j - \omega_j') a_j(t) \\ + \int_{V_M} d\mathbf{r} g_j N V_M^{-1} V_{r_i}(t) \exp[i(\omega_j' t - \mathbf{k}_j \cdot \mathbf{r})]. \end{aligned} \quad (3)$$

We note that  $\omega_j' \neq \omega_j$ , in general, because of the atom-field interaction.

For many quantum-optics problems, given the input state to the medium at  $z=0$ , we want to find the output state after paraxial propagation through the medium at

$z=L_M$ . We have dealt with this problem of spatial propagation of quantum fields by two different methods. In the quantum-mode method we utilize the solutions of Eq. (3) to obtain an approximate expression for the  $c$ -number electric field variable  $E(z,t)$ . If we assume the initial condition that  $a_j(t=0)=0$  for all  $j \neq m$ , we can then make the quasimonochromatic approximation and employ the paraxial-wave treatment. This initial condition implies that, at  $z=0$ , the wave going into the medium is oscillating at frequency  $\omega_m$  for  $t \geq 0$ , thereby exciting a quasimonochromatic field  $E_m(z,t)$  of nominal frequency  $\omega_m$  propagating in the region  $z > 0$ . Because of the integration over the finite size of the medium in Eq. (3), the input mode amplitude  $a_m$  is coupled to the amplitudes of those modes with  $\omega_j \approx \omega_m$ . Spatial propagation thus arises from the temporal evolution of many modes  $\{a_j(t)\}$  around the mode  $a_m(t)$ . Propagation of a multimode input field is obtained via  $E(z,t) = \sum_m E_m(z,t)$  for  $z > 0$ .

In the slowly varying-envelope method, we expand the field operator  $\hat{E}(z,t)$  in terms of modal operators  $\{\hat{a}_m(z,t)\}$ . Appropriate initial conditions are imposed on the commutation relations for  $\hat{a}_m(z,t)$  and  $\hat{a}_m^\dagger(z,t)$  so as to generate correct commutators for the field  $\hat{E}(z,t)$  at  $t=0$ . Unlike the quantum-mode method the frequencies  $\{\Omega_m\}$  of the mode functions  $\{\exp[-i(\Omega_m t - K_m z)]\}$  are predefined by periodic boundary conditions in time, and their wave-vector magnitudes  $\{K_m'\}$  are such that  $\{\hat{a}_m(z,t)\}$  are slowly varying in space. Using the operator wave equation and applying the usual slowly varying-envelope approximation, we obtain an equation of motion for  $\hat{a}_m(z,t)$ ,

$$\frac{\partial \hat{a}_m}{\partial z} + c_m \frac{\partial \hat{a}_m}{\partial t} = \mathcal{F}(\{\hat{\mathcal{P}}_m, (\partial/\partial t)\hat{\mathcal{P}}_m\}), \quad (4)$$

where  $\{c_m\}$  are constants and  $\{\hat{\mathcal{P}}_m(z,t)\}$  are slowly varying operators giving the medium polarization operator  $\hat{P}(z,t)$  in terms of the mode functions. Equation (4) can be converted to an equivalent  $c$ -number equation with the  $c$ -number variable  $P(z,t)$  obtained from  $V_{r_i}(t)$ , which in turn can be written in terms of the  $\{a_m(z,t)\}$  and their first derivatives  $\{(\partial/\partial t)a_m(z,t)\}$  as mentioned before. Thus, in the steady state where  $(\partial/\partial t)a_m(z,t)=0$ , a set of spatial coupled-mode equations for  $a_m(z,t)$  are obtained. This formalism only requires that  $(\partial/\partial z)a_m \ll |K_m'| a_m$  which is much less stringent than the adiabatic assumption  $(\partial/\partial t)a_m \ll \gamma_{\perp} a_m$  required by the heuristic  $t \rightarrow z/c$  transformation used in the earlier works.<sup>3</sup> Finally, although the two methods of spatial propagation are quite different, they give the same results.

Quantum field propagation has been treated previously in a serious manner, e.g., using a Schrödinger-picture wave packet,<sup>7</sup> or a slowly varying field envelope,<sup>8</sup> or a localized momentum operator.<sup>9</sup> Our slowly varying-envelope method differs from these previous treatments in that it is much more general. For example, it is valid even without the rotating-wave approximation, so it can be used to treat propagation at frequencies far removed from atomic resonance, as in the case of a transparent medium with real refractive index studied from the point of view of interaction with the atoms. Our quantum-mode method is less general, nevertheless, it treats multibeam interaction

and propagation in a medium by making direct use of the equation of motion for the annihilation operators. This method enables us to show, in a manner that has not been done in any previous treatment, how the temporal evolution of the annihilation operators gives rise to spatial propagation and diffraction.

We have applied the above formalism to the case of a single beam propagating through the medium along the  $z$  direction. The traveling wave consists of a strong pump component at frequency  $\Omega_p$ , arbitrarily detuned from  $\omega_a$ , and two weak probe and conjugate components at frequencies  $\Omega_m$  and  $\Omega_{-m}$ , respectively. Interaction occurs as the beam propagates through the medium if the phase-matching condition  $2\mathbf{K}'_p \approx \mathbf{K}'_m + \mathbf{K}'_{-m}$  is satisfied. Energy conservation requires that  $(\Omega_m - \Omega_p) = (\Omega_p - \Omega_{-m})$ . Using the slowly varying-envelope method, we obtain the following spatial coupled-mode equations:

$$\frac{\partial a_m}{\partial z} = -i\tilde{\gamma}_m a_m + \tilde{\chi}_m \exp(i\delta K'_m z) a_{-m}^\dagger + \tilde{\Gamma}_m, \quad (5a)$$

$$\frac{\partial a_{-m}^\dagger}{\partial z} = i\tilde{\gamma}_{-m}^* a_{-m}^\dagger + \tilde{\chi}_{-m}^* \exp(-i\delta K'_{-m} z) a_m + \tilde{\Gamma}_{-m}^\dagger, \quad (5b)$$

where  $\{\tilde{\gamma}_m, \tilde{\gamma}_{-m}\}$  and  $\{\tilde{\chi}_m, \tilde{\chi}_{-m}\}$  are the dispersion and the nonlinear-mixing coefficients, respectively, which agree with those obtained via the semiclassical theory.<sup>10</sup> Here

$$\delta K'_m \equiv (\mathbf{K}'_m + \mathbf{K}'_{-m} - 2\mathbf{K}'_p) \cdot \mathbf{e}_z$$

gives the phase mismatch between the pump and the probe-conjugate components, and  $\{\tilde{\Gamma}_m, \tilde{\Gamma}_{-m}\}$  are the noise terms, which correctly reproduce the resonance-fluorescence intensity spectrum<sup>11</sup> and the resonance-fluorescence squeezing spectrum as given by Collett, Walls, and Zoller.<sup>2</sup>

Equations (5) can be solved *analytically* giving the quadrature noise spectrum at the output of the medium for a variety of possible experimental parameters of which we illustrate only a few cases here. We denote the normalized pump detuning from the atomic resonance by  $\Delta_p \equiv (\omega_a - \Omega_p)/\gamma_\perp$  and the normalized probe detuning from the pump by  $\delta_m \equiv (\Omega_m - \Omega_p)/\gamma_\perp$ . The degenerate situation,  $\delta_m = 0$ , is plotted in Fig. 1, where the quadrature noise variance<sup>12</sup>

$$\delta \hat{X}_1^2(\theta) \equiv \langle [\hat{X}_1(\theta) - \langle \hat{X}_1(\theta) \rangle]^2 \rangle$$

is shown as a function of the normalized pump intensity  $\beta = \Omega_R/\gamma_\perp$ . Here  $\Omega_R$  is the Rabi frequency and the noise variance below the coherent-state value of  $\frac{1}{4}$  implies squeezing. The phase  $\theta$  which defines the quadrature amplitudes is referenced to the phase of the pump field and varied at each value of  $\beta$  to obtain minimum noise variance. Curve A is plotted for the collisionless case, i.e.,  $F=1$  with  $\Delta_p=100$  and  $a_0 L_M=10^4$ , where  $a_0$  is the unsaturated on-resonance absorption coefficient. To compare our results with those of Reid and Walls,<sup>3</sup> curve B is plotted with the same parameters as curve A but without inclusion of the pump-probe phase mismatch, i.e., by setting  $\delta K'_0=0$ . As can be seen, the inclusion of the pump-probe phase mismatch reduces the maximum amount of squeez-

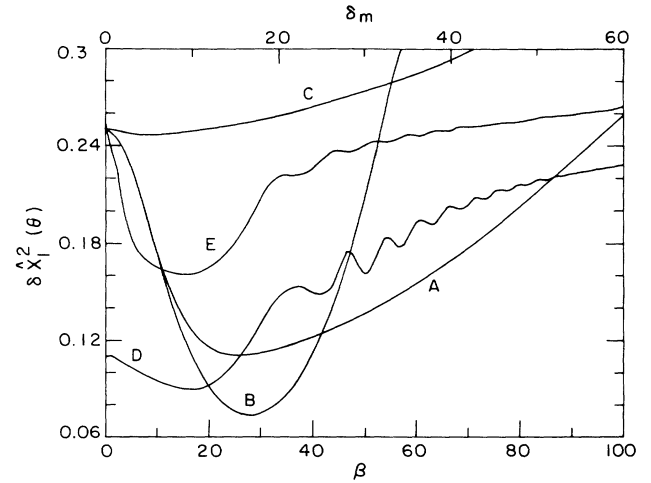


FIG. 1. Curves A, B, and C are plots of  $\delta \hat{X}_1^2(\theta)$  vs  $\beta$  in the degenerate limit with  $\Delta_p=100$  and  $a_0 L_M=10^4$ . A:  $\delta K'_0 \neq 0$  and  $F=1$ ; B:  $\delta K'_0=0$  and  $F=1$ ; C:  $\delta K'_0 \neq 0$  and  $F=0.2$ . Curves D and E show the squeezing spectra, i.e.,  $\delta \hat{X}_1^2(\theta)$  vs  $\delta_m$  (marked on the top abscissa) for  $\Delta_p=100$ ,  $\beta=26$ , and  $a_0 L_M=10^4$ . D:  $F=1$ , and for E:  $F=0.2$ .

ing achievable but broadens the range of pump intensity over which squeezing occurs. The effect of collisions on squeezing is shown in curve C which is plotted with the same parameters as curve A except for  $F=0.2$ .

The nondegenerate situation is depicted in Figs. 2 and 3 where the squeezing spectra are shown by plotting  $\delta \hat{X}_1^2(\theta)$  as functions of  $\delta_m$  for various cases of interest. Once again, in each case  $\theta$  is varied at each value of  $\delta_m$  to achieve minimum noise. Figure 2 shows the squeezing spectra for different values of  $a_0 L_M$  with  $\Delta_p=100$ ,  $\beta=100$ , and  $F=1$ . At low values of  $a_0 L_M$  (curve A), significant squeezing occurs only in the vicinity of the normalized generalized Rabi frequency  $\Delta_R \equiv (\Delta_p^2 + \beta^2)^{1/2}$ . As  $a_0 L_M$  is increased (curve B), the region of maximum

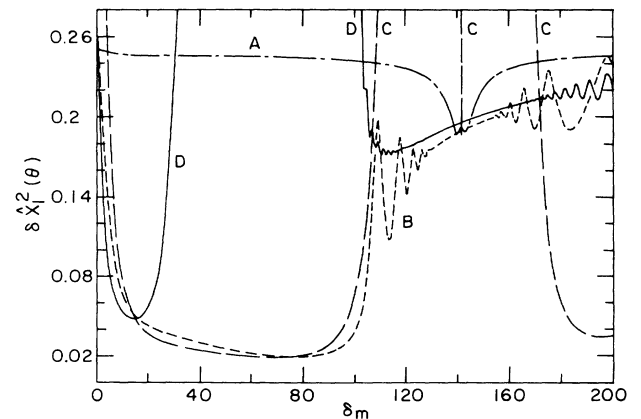


FIG. 2. Various squeezing spectra with  $\Delta_p=100$ ,  $\beta=100$ , and  $F=1$ . Curve A:  $a_0 L_M=5$ ; B:  $a_0 L_M=800$ ; C:  $a_0 L_M=800$  with  $\delta K'_m=0$ ; D:  $a_0 L_M=4 \times 10^3$ .

squeezing shifts toward lower values of  $\delta_m$ . The oscillations in the squeezing spectrum near  $\Delta_R$  are due to our inclusion of the pump-probe phase mismatch in those calculations. As shown in curve C, which is plotted with the same parameters as curve B but with  $\Delta K'_m$  set equal to zero, these oscillations disappear and no squeezing occurs in the vicinity of  $\Delta_R$ , except for a dip at  $\Delta_R$ . As  $\alpha_0 L_M$  becomes very large, a broad region of no squeezing appears below  $\Delta_R$  without significantly affecting the squeezing level near  $\Delta_R$ .

Figure 3 shows the squeezing spectra for different values of  $\beta$  with  $\Delta_p = 100$ ,  $\alpha_0 L_M = 4 \times 10^3$ , and  $F = 1$ . For  $\beta = 25 < \Delta_p$  (curve A), there is squeezing at the degenerate frequency which disappears for  $\beta \geq \Delta_p$  (curves B, C, and D) in accord with the degenerate theory of Reid and Walls.<sup>3</sup> On the other hand, *squeezing actually improves at nondegenerate frequencies as  $\beta$  increases beyond  $\Delta_p$*  as shown by curves C and D. Squeezing by a factor of  $> 10$  is possible at  $\delta_m \approx 130$  for  $\beta = 300$ .

Finally, in Fig. 1 (curves D and E), we illustrate the effect of collisions on the squeezing spectrum in the nondegenerate situation. Curve D is plotted with  $\Delta_p = 100$ ,  $\beta = 26$ ,  $\alpha_0 L_M = 10^4$ , and  $F = 1$  whereas in curve E,  $F$  is reduced to 0.2. Comparing curves D and E, we see that *although collisions reduce the amount of squeezing achievable for all  $\delta_m$ , the effect is very pronounced only at the degenerate frequency*. This is also evident in the change from curve A to curve C where the same change in the collision parameter ( $F = 1$  to  $F = 0.2$ ) almost completely destroys squeezing for all values of  $\beta$ .

The few cases illustrated above show the sensitivity of

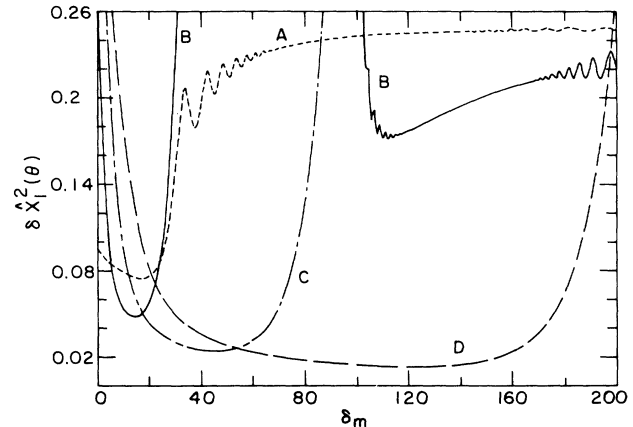


FIG. 3. Various squeezing spectra for different values of  $\beta$  with  $\Delta_p = 100$ ,  $\alpha_0 L_M = 4 \times 10^3$ , and  $F = 1$ . Curve A:  $\beta = 25$ ; B:  $\beta = 100$ ; C:  $\beta = 200$ ; D:  $\beta = 300$ .

the squeezing spectrum on the choice of parameters, which arises due to a complex inseparable interplay between the squeezing due to the fluorescing field<sup>2</sup> and that due to four-photon mixing.<sup>3</sup> The details of the theory, including propagation and its application to various squeezed-state generation schemes, will be described in a series of forthcoming publications.

This work was supported in part by the National Science Foundation under Grant No. 8415580.

\*Present address: Department of Electrical Engineering and Computer Science, Northwestern University, Evanston, IL 60201.

<sup>1</sup>M. W. Maeda, P. Kumar, and J. H. Shapiro, Phys. Rev. A **32**, 3803 (1985); Opt. Lett. **12**, 161 (1987).

<sup>2</sup>D. F. Walls and P. Zoller, Phys. Rev. Lett. **47**, 709 (1981); R. Loudon, Opt. Commun. **49**, 24 (1984); M. J. Collett, D. F. Walls, and P. Zoller, *ibid.* **52**, 145 (1984); A. Heidmann and S. Reynaud, J. Phys. (Paris) **46**, 1937 (1985).

<sup>3</sup>M. D. Reid and D. F. Walls, Phys. Rev. A **31**, 1622 (1985).

<sup>4</sup>M. D. Reid and D. F. Walls, Phys. Rev. A **33**, 4465 (1986); J. R. Klauder, S. L. McCall, and B. Yurke, *ibid.* **33**, 3204 (1986); D. A. Holm, M. Sargent III, and B. A. Capron, Opt. Lett. **11**, 443 (1986).

<sup>5</sup>R. E. Slusher, L. W. Hollberg, B. Yurke, J. C. Mertz, and

J. F. Valley, Phys. Rev. Lett. **55**, 2409 (1985).

<sup>6</sup>W. H. Louisell, *Quantum Statistical Properties of Radiation* (Wiley, New York, 1973).

<sup>7</sup>J. Tucker and D. F. Walls, Phys. Rev. **178**, 2036 (1969).

<sup>8</sup>F. Haake, H. King, G. Schröder, J. Haus, and R. Glauber, Phys. Rev. A **20**, 2047 (1979).

<sup>9</sup>Y. R. Shen, Phys. Rev. **155**, 921 (1967).

<sup>10</sup>T. Fu and M. Sargent III, Opt. Lett. **4**, 366 (1979); R. W. Boyd, M. G. Raymer, P. Narum, and D. J. Harter, Phys. Rev. A **24**, 411 (1981).

<sup>11</sup>B. R. Mollow, Phys. Rev. **188**, 1969 (1969); H. J. Kimble and L. Mandel, Phys. Rev. A **13**, 2123 (1976).

<sup>12</sup>This variance can be measured via homodyne-detection spectrum analysis, as in Ref. 1.